Provided for non-commercial research and education use.
Not for reproduction, distribution or commercial use.


This article appeared in a journal published by Elsevier. The attached copy is furnished to the author for internal non-commercial research and education use, including for instruction at the authors institution and sharing with colleagues.

Other uses, including reproduction and distribution, or selling or licensing copies, or posting to personal, institutional or third party websites are prohibited.

In most cases authors are permitted to post their version of the article (e.g. in Word or Tex form) to their personal website or institutional repository. Authors requiring further information regarding Elsevier's archiving and manuscript policies are encouraged to visit:

http://www.elsevier.com/copyright

Author's personal copy

Journal of Power Sources 196 (2011) 1461–1468

Contents lists available at ScienceDirect

Journal of Power Sources

journal homepage: www.elsevier.com/locate/jpowsour

# Copper sulfates as cathode materials for Li batteries

Jonathan N. Schwieger, Alexander Kraytsberg, Yair Ein-Eli*

*Technion Israel Institute of Technology, Department of Materials Engineering, Technion City, Haifa 32000, Israel*

ARTICLE INFO

*Article history:*
Received 12 May 2010
Received in revised form 8 July 2010
Accepted 29 July 2010
Available online 6 August 2010

*Keywords:*
Lithium batteries
Cathode material
Copper sulfate
Extrusion
Displacement reaction
Hydration water content

ABSTRACT

As lithium battery technology sets out to bridge the gap between portable electronics and the electrical automotive industry, cathode materials still stand as the bottleneck regarding performances. In the realm of highly attractive polyanion-type structures as high-voltage cathode materials, the sulfate group $(SO_4)^{2-}$ possesses an acknowledged superiority over other contenders in terms of open circuit voltage arising from the inductive effect of strong covalent S–O bonds. In parallel, novel lithium insertion mechanisms are providing alternatives to traditional intercalation, enabling reversible multi-electron processes securing high capacities. Combining both of these advantageous features, we report here the successful electrochemical reactivity of copper sulfate pentahydrate ($CuSO_4{\cdot}5H_2O$) with respect to lithium insertion via a two-electron displacement reaction entailing the extrusion of metallic copper at a dual voltage of 3.2 V and 2.7 V followed by its reversible insertion at 3.5 V and 3.8 V. At this stage, cyclability was still shown to be limited due to the irreversible degradation to a monohydrate structure owing to constitutional water loss.

© 2010 Elsevier B.V. All rights reserved.

## 1. Introduction

The increasing demand for enhanced energy-storage devices in the last three decades has propelled the electrochemical sciences, and lithium-ion technology with it, to the forefront of today's research. The electrochemical process employed by Li-ion batteries has been widely reported as intercalation; however such a process appears to be inherently limited to the transfer of a single electron per redox center, essentially restricting the achievable capacity and consequently the use of this technology to higher end applications [1]. In answer to this restraint, novel mechanisms have been gaining substantial momentum, supported by reversible changes in oxidation state by more than unity of a given transition metal, often leading to its electrochemical extrusion, thereby providing considerable capacity gains. The presence of such processes, namely conversion or displacement reactions, has been demonstrated in a variety of compounds from intermetallics such as $Cu_6Sn_5$ and $Cu_2Sb$ [2,3], as well as $AgMo_6S_8$ better known as Chevrel Phase [4], to covalent compounds such as oxides ($Co_3O_4$ [5,6]) and sulfides ($CoS_{0.89}$ and NiS [7]). However, the demonstrated operating voltages in many of these compounds are not high enough to efficiently compete with contemporary intercalation-based cathode materials derived from polyanion-type structures such as $LiFePO_4$ [8]. In these compounds, formulated as $M_x(XO_4)_y$, it was suggested that the inductive effect of the $(XO_4)^{n-}$ tetrahedral groups diminishes the energy of the metal redox couple relative to its simple oxide form, producing a higher operating voltage. The counter-cation X is crucial within such a structure as it shares a common oxygen atom with the metal through M–O–X linkages, directly influencing the achievable voltage. From studies relating to lithium insertion in $Fe_2(XO_4)_3$ frameworks, where X = W, Mo, S, it was inferred that the $(SO_4)^{2-}$ complex competitively produced 0.6 V higher open circuit voltages (OCV) that its runner-ups [9–11]. Aside from iron-based investigations, with a recent revival by Recham et al. on the synthesis and electrochemical properties of a lithiated fluorosulfate [12], and to the best of our knowledge, no electrochemical study has been carried out on sulfate-based cathode materials for Li battery technology with another transition metal.

From the past few years of research into conversion and displacement reactions, the M–V–O vanadate system with M=Cu has acquired considerable momentum due to the success of $Cu_{2.33}V_4O_{11}$ [13], among others [14,15], to reversibly extrude copper from the matrix with maximal capacities of 250–270 mAh $g^{-1}$ at voltages of 2.7 V or lower. Other copper-based compounds, namely copper sulfide, have been shown to exhibit a similar $Cu^{2+}/Cu^0$ redox couple providing high capacities albeit with reversibility issues and a lower potential [16]. In consequence, it is the aim of this study to combine the versatility of copper as a dual-electron exchange transition metal with the calculated superiority of the $(SO_4)^{2-}$ complex in a polyanion structure and to demonstrate the electrochemical performance of a simple resulting compound, copper sulfate.

As a mineral, copper sulfate is mostly encountered in nature in its pentahydrate form; it does nevertheless exist in a variety of other less stable hydration states (tri- and monohydrate) and an

* Corresponding author. Tel.: +972 4 829 4588; fax: +972 4 829 5677.
*E-mail address:* eineli@tx.technion.ac.il (Y. Ein-Eli).

0378-7753/$ – see front matter © 2010 Elsevier B.V. All rights reserved.
doi:10.1016/j.jpowsour.2010.07.090

Author's personal copy



anhydrous form. From electrochemical investigations into various hydrated compounds, namely $FePO_4{\cdot}nH_2O$ [17] and $FeVO_4{\cdot}nH_2O$ [18], the presence of constitutional water was not reported to hinder the intercalation mechanism of lithium. Consequently, the theoretical capacities expected for $CuSO_4{\cdot}5H_2O$ and $CuSO_4$ for a two-electron process are 215 mAh $g^{-1}$ and 336 mAh $g^{-1}$, respectively. Within the scope of this study, we report our findings on the electrochemical behavior of $CuSO_4{\cdot}nH_2O$ ($n$ = 0, 1, 5) *vis-à-vis* a conversion/displacement-based lithium insertion mechanism leading to the extrusion of metallic copper from the lattice. The focus of this investigation is set on the reversibility of this process, the effect of constitutional $H_2O$, as well as the optimization of the material's performances.

## 2. Experimental

$CuSO_4{\cdot}5H_2O$ and $CuSO_4$ anhydrous were purchased from Riedel–de Häen and Merck, respectively and used as received. Size reduction of the particles before casting of electrodes was carried out by grinding, sieving with three mesh sizes (149 μm, 99 μm and 53 μm), and/or ball-milling in a planetary mill (Torrey Hills Technologies) for various amounts of time at a speed of 140 rpm. Composite C–$CuSO_4{\cdot}nH_2O$ ($n$ = 0, 5) cathodes were prepared by mixing the active material with a binder (PVDF, Aldrich) and carbon black (Alfa Aesar) with a ratio of 80:10:10 of the three components respectively. Preparation of the slurry was either performed by simultaneously combining the $CuSO_4{\cdot}nH_2O$, PDVF and carbon (termed P1 preparation) or by previously ball-milling $CuSO_4{\cdot}nH_2O$ and carbon together (dispersed in $n$-hexane) then subsequently adding the binder (termed P2 preparation). *N*-methyl-2-pyrrolidone (Fluka) was added drop by drop into the mix to form a homogenous free-flowing paste. This slurry was then cast with a doctor blade set to produce a film thickness of 35 or 20 μm onto aluminum foil as current collector and set to dry in a vacuum oven at 110 °C for a period of 3 h, 48 h or 68 h. The foil was then punched into 1.2 $cm^2$ disks for electrochemical testing.

Special care was taken in the preparation of anhydrous $CuSO_4$ electrodes as to avoid rehydration of the powder in contact with ambient air. After receiving the chemical, it was stored in an MBRAUN glove box filled with 99.999% purity argon and with moisture and oxygen contents maintained below 10 ppm. All steps involved in the preparation of the slurry, except drying of the cast electrode in the vacuum oven, were handled inside the glove box, as well as sealing and re-opening of the container before and after ball-milling. The final $CuSO_4$ electrodes were therefore also stored in the glove box, as opposed to the pentahydrate electrodes kept in air.

Swagelok® T-connections were used as electrochemical cells and assembled in the glove box. Lithium metal foil was used as anode, and reference electrode when needed, Whatman grade 2 filter paper as the separator and 1 M $LiPF_6$ in EC:DMC (1:1 vol.%) as electrolyte (Novolyte Technologies). Galvanostatic electrochemical tests were performed on a MACCOR (model 2200), as well as Arbin (BT2000) battery cycler in a voltage range between 2.5 V and 4.0 V versus $Li/Li^+$, while slow scan cyclic voltammetry was carried out at a step rate of 0.05 mV $s^{-1}$ (in the same potential range as above) on a Princeton Applied Research Potentiostat/Galvanostat Model 273A equipped with PowerSuite software.

Characterization of the powders, as well as the composite electrodes and lithium foil before and after cycling was conducted by X-ray diffraction and SEM/EDS elemental analysis. XRD data was collected from a Philips Analytical X-ray with Cu Kα radiation operating at 40 kV/40 A. Electron microscopy studies were performed using a scanning electron microscope (FEI E-SEM Quanta 200) equipped with energy-dispersive X-ray spectroscopy (EDS). Crystal structure information was obtained from the ICSD database through the crystalOgraph applet available at lcr.epfl.ch and the 3D representations were constructed with the help of *Diamond* software. Additionally, water content of the electrolyte was measured by Karl–Fisher titration on a Metrohm Inc. 562 titrator.

## 3. Results and discussion

To evaluate the presence of electrochemical reactivity in a C–$CuSO_4{\cdot}nH_2O$/Li cell, preliminary galvanostatic experiments were performed on electrodes for both the anhydrous and pentahydrate form. These electrodes were prepared by grinding the active material to ensure homogeneity, mixing it together with a binder as well as 10 wt% carbon additive (P1 preparation) then cast to a thickness of 35 μm, generating an active material mass in the range of 4.5–5.5 mg in the punched cathodes, and finally dried for 3 h at 110 °C. Results from these experiments are displayed in Fig. 1. Whereas the anhydrous copper sulfate exhibits essentially no reactivity with lithium, barely interacting with 1/100th Li per formula unit over three cycles (Fig. 1a), the pentahydrate variant demonstrates the ability to insert approximately 1.5 Li per formula unit corresponding to a capacity equivalent of 156 mAh $g^{-1}$. The entire electrode samples run from this preparation exhibited the same

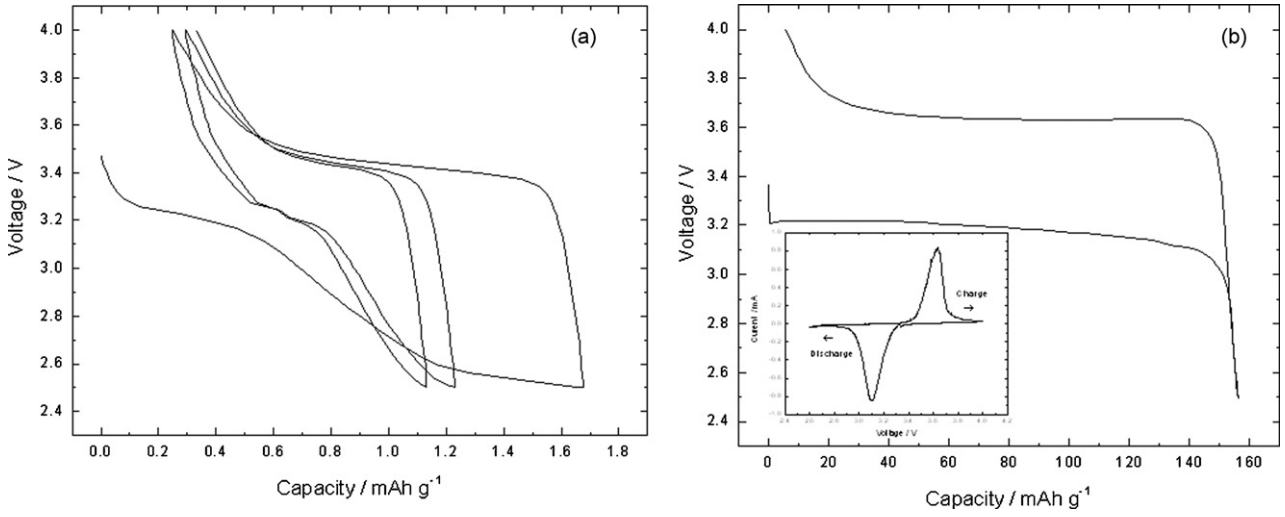


**Fig. 1.** Galvanostatic cycling of (a) anhydrous $CuSO_4$ (3 cycles at 9.5 mAh $g^{-1}$) and (b) $CuSO_4{\cdot}5H_2O$ (1 cycle at 23.1 mAh $g^{-1}$) from electrodes prepared by grinding of active material (P1 preparation, 10 wt% carbon, dried for 3 h at 110 °C, 35 μm thickness). Inset (b) slow scan cyclic voltammogram of $CuSO_4{\cdot}5H_2O$.

Author's personal copy



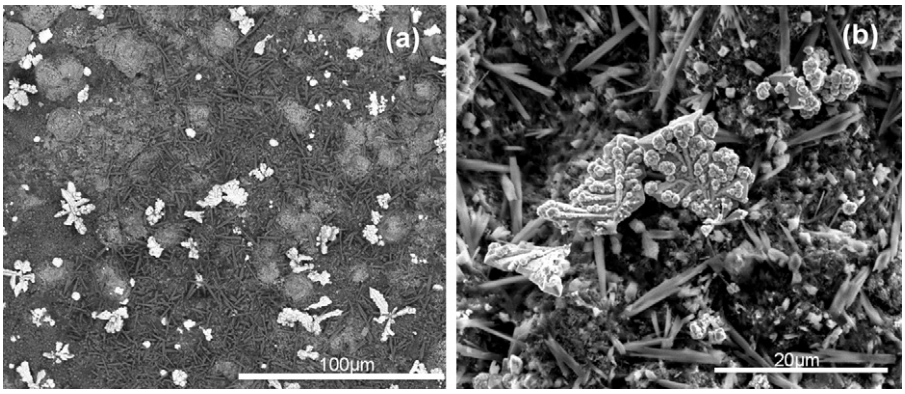


**Fig. 2.** SEM micrographs of a $CuSO_4{\cdot}5H_2O$ electrode (P1 preparation, 10 wt% carbon, dried for 3 h at 110 °C, 35 μm thickness) after initial discharge down to 2.5 V: (a) backscattered electron imaging mode, (b) close-up of metallic copper dendrite formation in secondary electron imaging mode.

behavior, i.e. a large initial discharge capacity with various degrees of recovery upon charge but failure to proceed any further producing this single-cycle capacity plot (Fig. 1b). The voltage range of electrochemical reactivity is quite high as excepted from the inductive effect of the polyanion structure: during discharge, insertion of lithium occurs near 3.2 V versus $Li/Li^+$ for both forms, while subsequent extraction takes place at 3.5 V for a hydration value $n = 0$ and at 3.65 V for $n = 5$. Furthermore, the presence of perfectly flat plateaus at operating potentials can be nicely noticed. In comparison to the copper-vanadate system, the cell potential reported here is 500 mV higher than what is obtained for $Cu_{2.33}V_4O_{11}$ (see [13]). A further examination of the electrochemical processes at hand was undertaken by cyclic voltammetry of copper sulfate pentahydrate with the same electrode preparation scheme (Fig. 1b inset). Two well-defined peaks can be seen at 3.10 V and 3.63 V versus $Li/Li^+$ on discharge and charge respectively, matching up with the values presented previously from galvanostatic experiments. Additionally, the symmetrical nature of the peaks is in good agreement with the 96% reversibility on the first cycle.

The apparent reaction taking place upon lithium insertion is demonstrated to be more than a simple one-electron process since approximately 1.5 Li were shown to be inserted previously. In order to validate our hypothesis of a conversion or displacement reaction replacing the traditional intercalation mechanism, characterization of the electrode after initial discharge down to 2.5 V was performed. Again, these tests were executed from the same casting conditions as detailed previously. Fig. 2 presents the SEM micrographs from the surface of the electrode once removed from the cell and dried of electrolyte. Under backscattered electron imaging mode, a phase clearly distinctive from the background matrix can be noticed (white in Fig. 2a) and was confirmed by EDS (see Fig. S1 in Supplementary Information) to be metallic copper deposits. The extrusion of the metal from the lattice, apparent from the dendrite-type formations bursting from the surroundings (Fig. 2b, center), is a clear confirmation of the expected two-electron process. Additionally, these micrographs provide insight into the type of process at hand, namely conversion or displacement. Indeed, while conversion reactions are characterized by the formation of fine nanoscale metallic deposits, displacement reactions extrude the metal into well-noticeable dendritic structures, as obtained here.

Having demonstrated the presence of the extrusion process, the lack of cyclability past the first charge of $CuSO_4{\cdot}5H_2O$ was investigated while its anhydrous counterpart was set aside temporarily. Optimization of the casting process was attempted firstly by targeting the size of the active material particles within the composite electrode [19,20]. To reduce the scale of the particles, pentahydrate copper sulfate was sieved down to 149 μm, 99 μm and 53 μm, cast as electrodes for these three sizes respectively (P1 preparation, 10 wt% carbon, dried for 3 h at 110 °C, 35 μm thickness) and cycled in a galvanostatic mode. Since no noticeable improvement was perceived, the particle size was shrunk further by switching to the P2 method, i.e. ball-milling of the active material with carbon. Electrodes were prepared by milling the ground and sieved (53 μm grid) active material for 12 h with 10 wt% carbon and cast with a thickness of 35 μm, then dried for 68 h at 110 °C. A comparison between the particle size of $CuSO_4{\cdot}5H_2O$ following sieving and ball-milling is presented in Fig. 3, clearly showing the micrometer-size range in the former (Fig. 3a) and the nanometer-size range in the latter (Fig. 3b).

With the nanometer scale particles produced via ball-milling, electrochemical tests were performed on these newly prepared

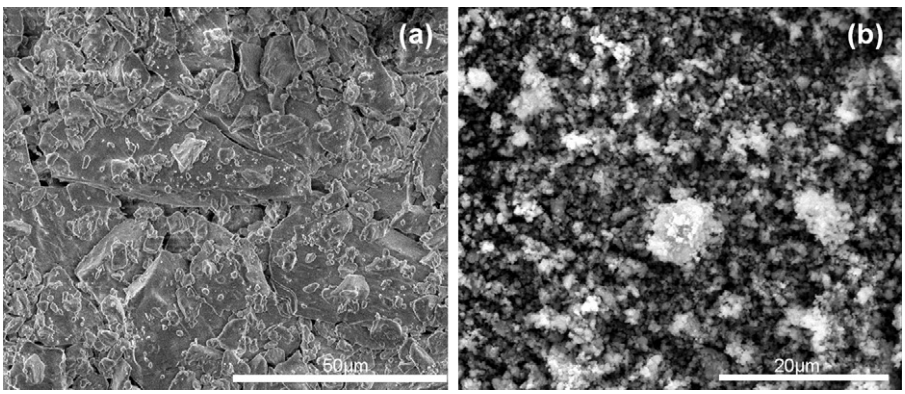


**Fig. 3.** SEM micrographs of $CuSO_4{\cdot}5H_2O$ particles: (a) sieved down to 53 μm, (b) sieved down to 53 μm followed by ball-milling for 12 h with 10 wt% carbon at 140 rpm.

Author's personal copy



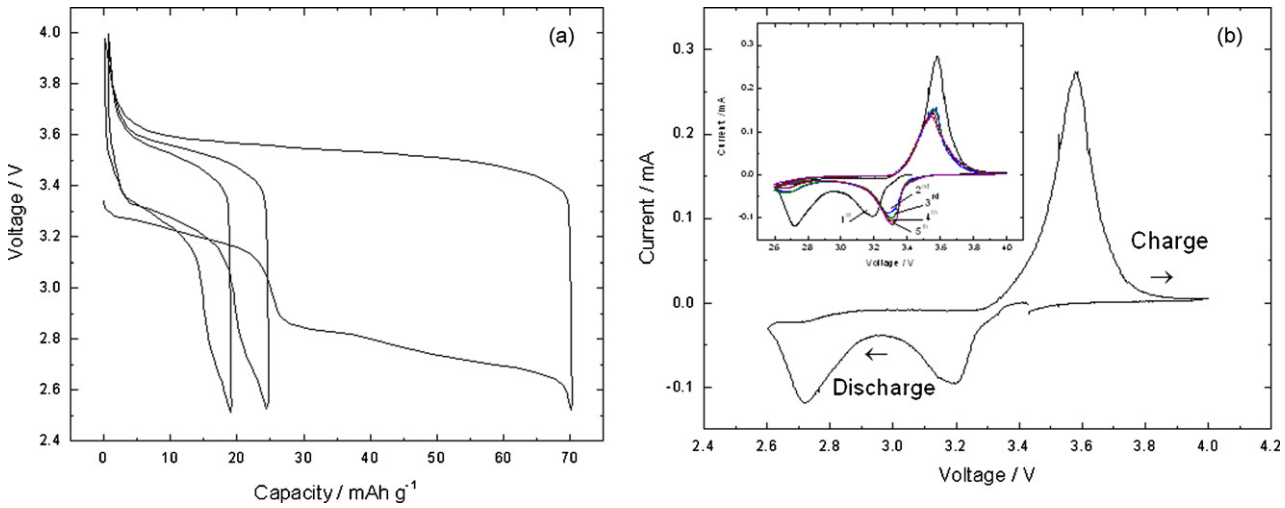


**Fig. 4.** Electrochemical tests on $CuSO_4 \cdot 5H_2O$ following size reduction of active material via ball-milling (electrodes: P2 preparation, 10 wt% carbon, dried for 60 h at 110 °C, 35 μm thickness): (a) galvanostatic cycling (3 cycles at 18.4 mAh $g^{-1}$), (b) slow scan cyclic voltammogram (1 cycle at 0.05 mV $s^{-1}$). Inset (b) slow scan cyclic voltammogram of cycles 1 through 5.

electrodes. The outcomes of these tests are displayed in Fig. 4. Consistent with our previous data (see Fig. 1), an initial operating potential along discharge can be noticed centered at 3.2 V while the charge plateau hovers in the vicinity of 3.6 V (Fig. 4a). Additionally though, a second plateau can be seen during the first discharge at a lower potential of 2.7–2.8 V, yet its amplitude diminishes drastically in further cycles. The combination of these two plateaus produces a discharge capacity of 70 mAh $g^{-1}$ (32% of the theoretical value). The cyclability is quite poor, as only 35% of the initial capacity is achieved in the second cycle and this value degrades further with cycle number. What can be noted as well is the excellent recovery upon charge with a value greater than 98% for the three shown cycles. Each of these features, i.e. double plateau throughout the first discharge, absence of this phenomenon in subsequent discharges and large initial capacity in comparison to following cycles, are all confirmed in the cyclic voltammetry experiment presented in Fig. 4b and inset. Indeed, the two peaks at 3.19 V and 2.72 V are clearly present in the first cycle, as opposed to the single peak in Fig. 1b (inset), while the second one disappears afterwards. Moreover, the CV curve shows an additional feature, also present in the cycling data but less noticeable: peak shifting to a higher potential from 3.19 V to 3.30 V after the first cycle.

To counteract the effect of capacity loss observed until now for copper sulfate in our ball-milled cells, reduction in active material mass was conducted by casting thinner electrodes to attempt to avoid unreacted material during cycling. New cathodes with a thickness of 20 μm corresponding to an active material content of 2–2.5 mg per disk were prepared (P2 preparation, 10 wt% carbon, dried for 48 h at 110 °C) and similar tests as above were run. Fig. 5 presents the data plotted in the same fashion as Fig. 4 for better comparison. For this final optimization, the galvanostatic and cyclic voltammetry results indicate the presence of a double process not only upon discharge, at 3.12 V and 2.70 V, but also upon charge where the previously single peak at 3.58 V is replaced by one at 3.53 V and one at 3.82 V. The expected increase in capacity retention was perceived to some extent, with 66% of the initial discharge value retained in the second cycle compared to 35% in the previous results. However, this value continues to degrade further as before and additionally the recovery upon charge of the accumulated capacity is 87% for the first cycle and decreases down to 70% already for the third cycle. The voltage spikes present at the beginning of the discharge processes are due to the current density applied and were eliminated at lower currents. An important point to notice is the persistence of the dual discharge and charge pro-

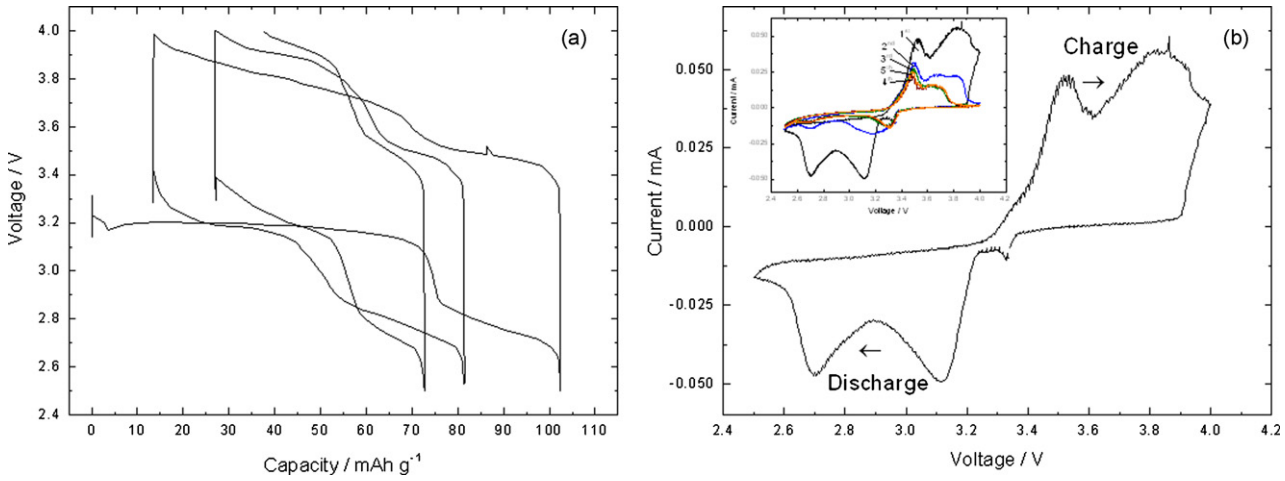


**Fig. 5.** Electrochemical tests on $CuSO_4 \cdot 5H_2O$ following size reduction of active material via ball-milling as well as thinning of electrodes (P2 preparation, 10 wt% carbon, dried for 48 h at 110 °C, 20 μm thickness): (a) galvanostatic cycling (3 cycles at 21.6 mAh $g^{-1}$)), (b) slow scan cyclic voltammogram (1 cycle at 0.05 mV $s^{-1}$). Inset (b) slow scan cyclic voltammogram of cycles 1 through 5.

Author's personal copy



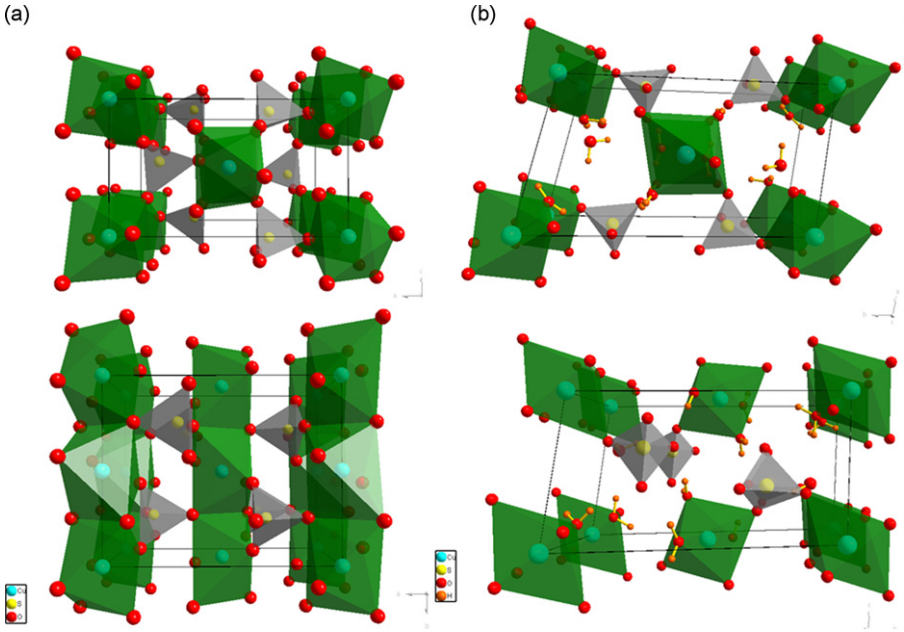


**Fig. 6.** Crystal structures of (a) $CuSO_4$ ($V = 272.7$ Å$^3$) viewed down the *b*-axis (top) and *c*-axis (bottom), as well as (b) $CuSO_4{\cdot}5H_2O$ ($V = 364.0$ Å$^3$) along the *c*-axis (top) and *a*-axis (bottom).

cesses past the first cycle. This fact was not noticed in our previous cells and is not clearly seen in the cyclic voltammetry data. Nevertheless, similarly as above, CV curves validate the loss of capacity from the first cycle on and demonstrate the same noted peak shift from 3.12 V to 3.30 V.

Our investigation so far was able to reveal the electrochemical activity of $CuSO_4$ pentahydrate but not of $CuSO_4$ anhydrous. As the basic difference between both of these compounds arises from their respective hydration state, a closer look into the crystal structures was taken. Fig. 6a and b presents the unit cell for both the anhydrous (orthorhombic cell, *Pnma* space group, $a = 8.409(1)$ (Å), $b = 6.709(1)$ (Å), $c = 4.839(1)$ (Å)) and pentahydrate (triclinic cell, $P\bar{1}$ space group, $a = 6.1224(4)$ (Å), $b = 10.7223(4)$ (Å), $c = 5.9681(4)$ (Å), $\alpha = 82.35(2)$, $\beta = 107.33(2)$, $\gamma = 102.6(4)$) compounds as viewed down different directions of the lattice with polyhedra shapes added in order to better visualize the arrangement of atoms and free space within the unit cell. The incorporation of five water molecules within the structure upon hydration clearly produces two essentially different structures. However, when considering the buildup of this lattice from a polyhedral perspective, the strong similarities in between both variants of copper sulfates are indubitably enhanced. While the anhydrous configuration is based on chains of edge-sharing $CuO_6$ octahedra densely interconnected by $SO_4$ tetrahedra, the pentahydrate possesses un-adjoining $CuO_6$ octahedra only sparsely connected by $SO_4$ groups (each octahedron links to two others via a tetrahedral group). The swelling of the structure due to hydration water is clearly felt in the representations below since the copper-centered octahedra as well as the sulfur-centered tetrahedra have similar dimensions in both structures (Cu–O bonds ranging from 1.92 Å to 2.38 Å, S–O bond from 1.45 Å to 1.52 Å) and the lattice parameters are augmented. The total volume increase is roughly 33%, from 272.7 Å$^3$ to 364.0 Å$^3$, hence this more spacious configuration is suspected to better accommodate the flow of lithium ions during cycling and thus enhance the performance. Such an effect has previously been demonstrated for another family of hydrated compounds, namely $WO_3{\cdot}nH_2O$ ($n = 1$, 2) based on a defected perovskite structure where the larger spacing in the $n = 2$ compound produced enhanced ion migration within its structure leading to improved electrochromic properties [21]. To further ascertain whether or not this difference could be responsible for such a dramatic change in reactivity with lithium, copper sulfate pentahydrate was dehydrated to a monohydrate state and investigated electrochemically. Powder samples were placed in a vacuum oven and dried for 48 h at 110 °C, then stored under argon atmosphere in a glove box to avoid rehydration in contact with air. Characterization of the resultant powder was performed by XRD on a sample wrapped in a protective cellophane film to avoid contact with ambient air. The diffraction pattern is presented in Fig. 7a where the peaks were identified as belonging to copper sulfate monohydrate (see Bragg positions) albeit with a low crystallinity of the compound. In Fig. 7b, the crystal structure for this compound is presented, again with polyhedral information. In comparison to anhydrous copper sulfate, the incorporation of one water molecule loosens the structure, noticeable by the loss of direct contact between $CuO_6$ octahedrons, however the total cell volume slightly decreases as apparent from the lattice parameters of the triclinic cell ($P\bar{1}$ space group): $a = 5.037(1)$ (Å), $b = 5.170(1)$ (Å), $c = 7.578(2)$ (Å), $\alpha = 108.62(1)$, $\beta = 108.39(1)$ and $\gamma = 90.93(1)$. To establish the connection between structure and performance, cast $CuSO_4{\cdot}5H_2O$ electrodes (10 wt% carbon, 20 μm thickness) were dehydrated following the same route as above, then stored under argon. A P2 preparation method was used to obtain a similarly optimized electrode as presented previously. Galvanostatic cycling data acquired from such an electrode is displayed in Fig. 7c. The poor performance of this cathode, where less than 5 mAh g$^{-1}$ of capacity are exchanged during the first three cycles, is quite similar to that of anhydrous copper sulfate, hence very poor in comparison to the pentahydrate compound; result which was to be expected from structural considerations due to absence of sufficient swelling of the lattice. The lack of substantial reactivity with lithium provides further ground to ascertain the pronounced positive effect of high levels of hydration water in $CuSO_4{\cdot}nH_2O$.

As presented previously, the performances of $CuSO_4{\cdot}5H_2O$ as a cathode material were seen to respond to the various optimization techniques put to use. Following a drastic reduction in particle size as well as thinning of the electrodes to restrict the amount of active material, the electrochemical process was observed to evolve from a single-step one on both discharge and charge to

Author's personal copy



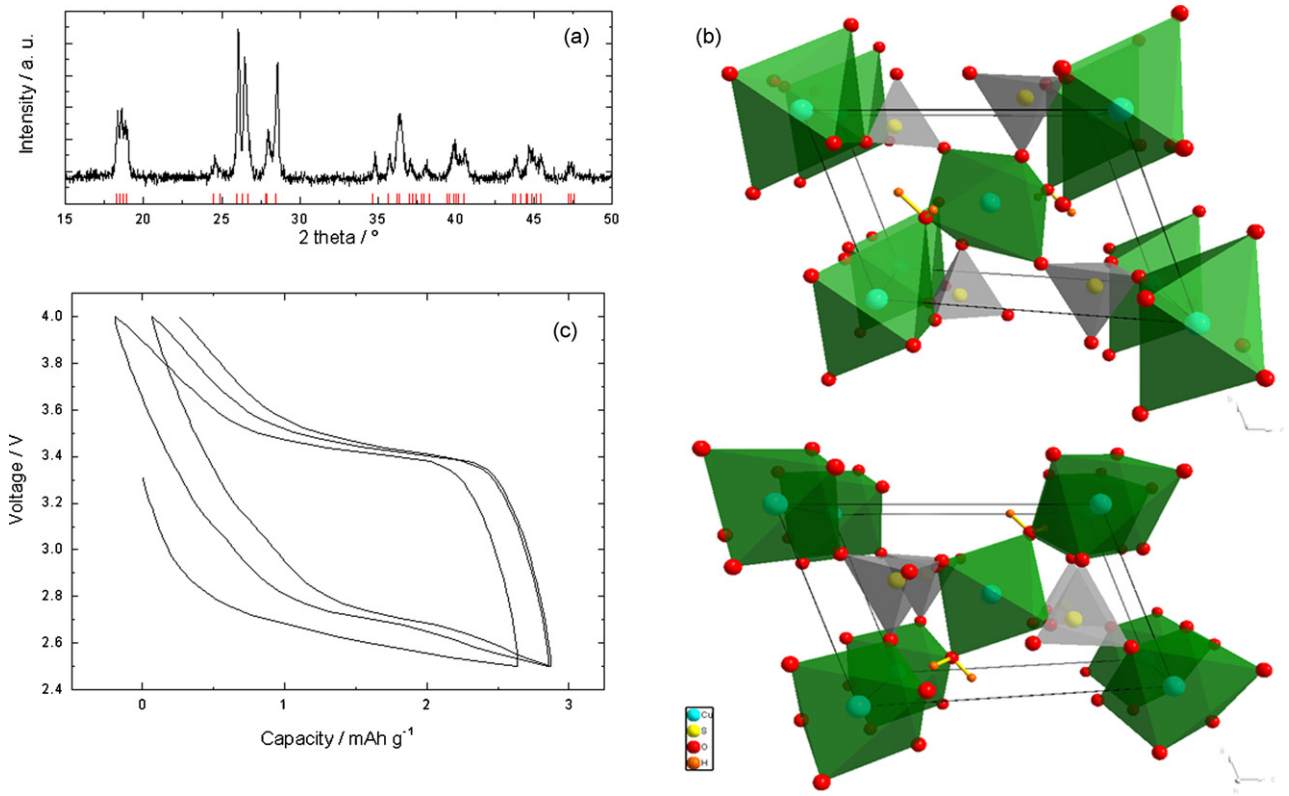


**Fig. 7.** Copper sulfate monohydrate structural and electrochemical data: (a) X-ray diffraction pattern of dehydrated $CuSO_4{\cdot}5H_2O$ with Bragg reflection positions (powder diffraction file 01-080-0392), (b) crystal structure representation of $CuSO_4{\cdot}H_2O$ along *a*-axis (top) and *b*-axis (bottom), (c) galvanostatic cycling of $CuSO_4{\cdot}H_2O$ electrode (P2 preparation, 10 wt% carbon, dried for 48 h at 110 °C, 20 μm thickness) at 32.7 mAh $g^{-1}$.

a two-step process in both of these stages. Such a size effect in Li-ion cathode materials was demonstrated by Kovacheva et al. in $LiNi_{0.5}Mn_{1.5}O_4$, where switching from micrometer-sized particles to nano-particles revealed two pairs of oxidation/reduction peaks at high voltages, instead of only one, corresponding to the $Ni^{2+}/Ni^{3+}$ and $Ni^{3+}/Ni^{4+}$ redox couples, respectively [22]. This behavior was attributed to the reduced migration distances as well as higher surface area available due to size reductions providing faster charge transfer kinetics and allowing higher resolution of the chrono-amperometric response of this material. Even though, this particular material reacts with lithium through an intercalation reaction whereas we have demonstrated the presence of a displacement mechanism in copper sulfate, the results obtained here can be explained through similar considerations. The overall redox process taking place was shown to be the extrusion of metallic copper from the lattice during discharge, $Cu^{2+} \rightarrow Cu^0$ and reinsertion during charge, $Cu^0 \rightarrow Cu^{2+}$, confirmed by the disappearance of the dendritic structures at 4 V (see Fig. 8). With electrodes cast from micro-particles, each of these processes takes place in a single-step whereas with nano-particles they were each suspected to occur in two steps for discharge, $Cu^{2+} \rightarrow Cu^{1+}$ (3.1–3.2 V) and $Cu^{1+} \rightarrow Cu^0$ (2.7 V), while for charge, $Cu^0 \rightarrow Cu^{1+}$ (3.5 V), and $Cu^{1+} \rightarrow Cu^{2+}$ (3.8 V).

This mechanism would imply the information of an intermediary compound in which copper is at +1 oxidation state. In order to confirm or infirm this, as well as clearly establish the processes involved during the extrusion/reinsertion of copper, X-diffraction analysis was carried out. At the present, we opted for an *ex situ* XRD analysis on our electrode material at various stages during the initial discharge/charge cycle: as-cast, after simple monitoring of OCV during a 24 h period (no cycling), discharged to 3.0 V, discharged to 2.5 V as well as a full 2.5–4.0 V cycle. Each of these five cathodes were then recuperated and scanned between $2\theta$ angles of 15–50°, the results of which are displayed in Fig. 8. Due to the *ex situ* character of this experiment, comparison between scans can only be performed in a qualitative fashion, leaving out quantitative information regarding phases present. Nonetheless, important insight can be extracted from these results. The as-cast electrode

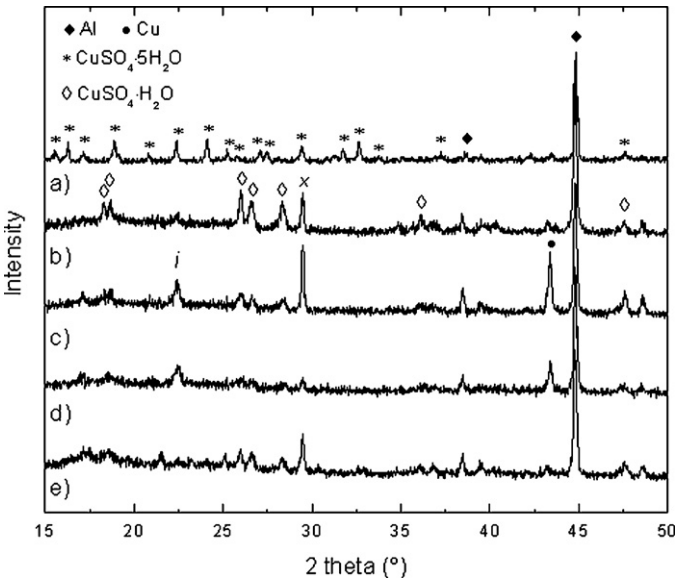


**Fig. 8.** X-ray diffraction data collected on $CuSO_4{\cdot}5H_2O$ electrodes at five different stages during the first cycle: (a) electrode as-cast, (b) cell with OCV monitoring for 24 h (no cycling), (c) cell discharged to 3.0 V at 26.1 mAh $g^{-1}$, (d) cell discharged to 2.5 V at 25.0 mAh $g^{-1}$, (e) cell discharged to 2.5 V and charged to 4.0 V for a full cycle at 25.0 mAh $g^{-1}$. Aluminum peaks from the current collector are indicated at $2\theta = 38.5°$ and 44.7°.

Author's personal copy



in Fig. 8a is presented for reference, with both the copper sulfate pentahydrate as well aluminum current collector peaks indicated. At this point, it is worthwhile to compare this particular data set to the XRD pattern of the pristine (non-ball-milled) material (see Fig. S2 in Supplementary Information). From this comparison an undeniable effect of the 12 h mechanical ball-milling was perceived on the structure of the active material in the electrode, namely a loss in crystallinity. Because the importance of the structure of $CuSO_4{\cdot}5H_2O$ was established earlier, this conclusion appears to explain the noted decrease in specific capacity of cells from Fig. 1 to Figs. 4 and 5.

Interestingly, the initial electrode structure appears to degrade in electrolyte after an extensive period of time, as demonstrated in Fig. 8b. Indeed, the original pentahydrate peaks have vanished while a monohydrate structure appears to be present, hinting towards an electrolyte-related water leakage of $CuSO_4{\cdot}5H_2O$. Karl Fisher titration was carried out on the electrolyte collected from this cell and revealed higher water content as compared to the nominal level in the electrolyte solution, confirming such degradation. During discharge, the general structure of the electrode can be seen to undergo an initial and similar transition to a monohydrate state at 3.0 V while abandoning this new structure to some extent when reaching 2.5 V. At both of these stages, an intermediary phase, most certainly an Li-based phase resulting from the insertion of $Li^+$ into the cathode, reasonably identified as $Li_2SO_4$, can be noted with a single peak at $2\theta = 22.5^\circ$, denoted *i*. Metallic copper is present at 2.5 V, as expected, but also at 3.0 V, clearly questioning our initial hypothesis of one-electron processes at each stage whereby $Cu^0$ deposits should only be noticed at the lower discharge potential. When extracting the inserted lithium during the charge process, both the intermediary *i* phase and extruded metallic copper disappear while leaving behind an apparently poorly crystallized copper sulfate monohydrate structure instead of the expected pentahydrate. Along this whole procedure, an additional peak can be noticed regardless of the degree of lithium insertion/extraction. Denoted *x*, it is explained by a preferential orientation phenomenon of the crystallized $CuSO_4{\cdot}5H_2O$ particles which arose while casting and drying the electrode and remains a structural feature throughout cycling. Because each of these diffraction patterns was collected at random orientations, the intensity of the *x* peak is simply representative of the alignment of the sample with respect to its preferred orientation.

This structural deterioration from interactions between $CuSO_4{\cdot}5H_2O$ and the electrolyte, or more specifically the organic solvent, is consistent with its dehydration mechanism. Indeed copper sulfate pentahydrate possesses two types of bonding between water molecules and the crystal, leading to four water molecules coordinated with a copper ion, forming with two sulfate groups a $CuO_6$ octahedron, and one bound to the structure solely by hydrogen bonds [23]. While the first four, bound as ligands, are evacuated from the structure during dehydration at temperatures below 150 °C, the last one requires temperatures upwards of 200 °C [24,25]. Hence, it comes as no surprise that in such organic electrolytes with a documented affinity towards water, the first four $H_2O$ water molecules would be extracted with relative ease, while the last one would remain coordinated within the structure, producing a monohydrate variant of copper sulfate. The degradation of the electrochemical performance can therefore be explained based on this loose water, which has a two-fold impact on the investigated cell. On one hand, from general considerations, reaction with water at the anode would lead to some poisoning of the surface with insoluble LiOH, restricting the availability of bulk lithium for electrochemical processes. On another hand, this leakage of coordinating water molecules inhibits the recrystallization of $CuSO_4{\cdot}5H_2O$ at the cathode after initial charge. Both of these phenomena, perhaps more importantly the latter, coupled with the effects of the long ball-milling periods highly affect the electrochemical reaction taking place, explaining the unachieved theoretical capacity and the low capacity retention upon subsequent cycling. The discrepancies between the first and latter cycles, such as capacity and potential shifts, also arise from these considerations, since the starting phases are not identical.

Additional investigations of cycled cells were carried out by examining the lithium anode under SEM and EDS which revealed the presence of copper deposits in both the discharged and charged states. These deposits, accumulated by corrosion of the copper dendrite formations at the cathode, poison the surface of the anode as well as restrict the achievable capacity in subsequent cycles since this copper is no longer available at the cathode. This side reaction is a common interaction of the electrolyte with such transition metals but water-contaminated electrolyte solutions have been reported to enhance such transition metal dissolution in similar compounds due to the presence of acidic contaminants, formed by the contact of $LiPF_6$ salts with loose water [26]. From the results of our analysis of cells interrupted at various stages of the first cycle, a suggested mechanism was established for the overall lithium insertion mechanism leading to the $Cu^{2+} \rightarrow Cu^0 \rightarrow Cu^{2+}$ process, and is displayed in Eqs. (1) and (2):

$$Cu^{2+}SO_4 \cdot 5H_2O \xrightarrow{+2Li^+ + 2e^-} xCu^{2+}SO_4 \cdot H_2O + (1-x)Cu^0 + 4H_2O$$
$$+ (1-x)I \xrightarrow{-2Li^+ - 2e^-} Cu^{2+}SO_4 \cdot H_2O + 4H_2O \quad (1)$$

$$2H_2O + 2Li \rightarrow 2LiOH + H_2 \quad (2)$$

Here, *I* is suspected to be $Li_2SO_4$.

The issue presently is that this mechanism, albeit accounting for the general process, does not successfully explain the dual insertion process presented by cycling data and confirmed by cyclic voltammetry. A similar discharge process has been noted in another copper-based extrusion compound investigated as anode material for lithium batteries, having Li insertion potentials of 1–1.5 V [27]. Upon galvanostatic discharge, copper (II) oxide (CuO) can exhibit two voltage plateaus depending on the morphology of the particles and environmental conditions such as temperature [27], while by collecting equilibrium potential curves this dual process becomes obvious [28]. This proven mechanism, attributed to the successive reduction of $Cu^{2+} \rightarrow Cu^{1+}$ and $Cu^{1+} \rightarrow Cu^0$, was extrapolated to our situation, coupled with a crucial assumption: the lack of an intermediary $Cu^{1+}$ compound arises from its instability in such a system, leading to a disproportionation reaction as in Eq. (3). Indeed, the partially discharged state displayed in Fig. 8c presents the simultaneous existence of $Cu^{2+}$ $SO_4{\cdot}H_2O$ and $Cu^0$, while *ex situ* experiments on CuO also revealed the presence of $Cu^0$ after the first plateau (see [28]).

$$2Cu^{1+} \rightarrow Cu^0_{(s)} + Cu^{2+} \quad (3)$$

As a general comparison to other hydrated materials investigated as cathode materials for lithium batteries where the insertion process can be viewed as intercalation, the complex extrusion mechanism renders consistent analogies quite complex therefore, evidencing the need to pursue and develop our understanding of the present processes which could lead to, if $CuSO_4{\cdot}5H_2O$ is viably cycled, a highly promising new cathode material for Li batteries.

## 4. Conclusions

In this investigation we reported the successful electrochemical reactivity of lithium with copper sulfate pentahydrate through a two-electron displacement reaction leading to the extrusion of metallic copper from the lattice. Flat operating voltage values in the 3 V range were demonstrated, as expected for polyanion-based

Author's personal copy



structures benefitting from an inductive effect. Whereas the pentahydrate variant benefits from an open structure with loosely interconnected $CuO_6$ groups, enabling lithium to proceed more readily within the lattice, both the anhydrous and monohydrate variant possess higher degrees of polyhedral connectivity reducing their respective electrochemical reactivity. By optimizing the preparation of the $CuSO_4{\cdot}5H_2O$ electrodes to reduce the size of the active particles, the electrochemical reaction was observed to evolve from a single-step process on both discharge and charge to a two-step process during each of these segments. While the complete understanding of this two-step process is assumed to be a disproportionation reaction, a plausible overall reaction was established from an analysis of partially discharged and charged cells, where the original copper sulfate pentahydrate matrix extrudes metallic copper leaving lithium sulfate behind while the remaining matrix is degraded by loss of water to a monohydrate state. The low capacity retention, 66% from first to second cycle, as well as unachieved theoretical capacity (47%) were explained by the loss in crystallinity of the material after ball-milling, the structural degradation at the cathode, the reaction of the lithium anode with water as well as the presence of copper deposits at the anode.

Mitigation of these harmful processes is essential to take full advantage of the highly attractive electrochemical features embodied by this material and propel it to practical applications. A viable way to do so is to consider variations on the $CuSO_4{\cdot}5H_2O$ compound in which hydration water is partially substituted with another polar molecule, such as $NH_3$, thereby purposely alleviating water removal from the lattice. This approach, currently investigated by our group, aims to demonstrate the improved reactivity versus lithium of a compound such as tetra-aminecopper (II) sulfate monohydrate, i.e. $Cu(NH_3)_4SO_4{\cdot}H_2O$, and confirm the viability of copper-based sulfates as cathode materials for lithium batteries.

## Acknowledgments

This research was financially supported by the Grand Technion Energy Program (GTEP), a joint grant from the Center of Absorption in Science of the Ministry of Immigrant Absorption and by the Committee for Planning and Budgeting of the Council for Higher Education under the framework of SHAPIRA Program.

## Appendix A. Supplementary data

Supplementary data associated with this article can be found, in the online version, at doi:10.1016/j.jpowsour.2010.07.090.

## References

[1] R. Malini, M. Uma, T. Sheela, M. Ganesan, N.G. Renganathan, Ionics 15 (2009) 301–307.
[2] K.D. Kepler, J.T. Vaughey, M.M. Thackeray, Electrochem. Solid State Lett. 2 (7) (1999) 307–309.
[3] L.M.L. Fransson, J.T. Vaughey, R. Benedek, K. Edström, J.O. Thomas, M.M. Thackeray, Electrochem. Commun. 3 (2001) 317–323.
[4] J.-M. Tarascon, T.P. Orlando, M.J. Neal, J. Electrochem. Soc. 135 (4) (1988) 804–808.
[5] M.M. Thackeray, S.D. Baker, K.T. Adendorff, J.B. Goodenough, Solid State Ionics 17 (1985) 175–181.
[6] D. Larcher, G. Sudant, J.-B. Leriche, Y. Chabre, J.-M. Tarascon, J. Electrochem. Soc. 149 (3) (2002) A234–A241.
[7] A. Débart, L. Dupont, R. Patrice, J.-M. Tarascon, Solid State Sci. 8 (2006) 640–651.
[8] A.K. Padhi, K.S. Nanjundaswamy, J.B. Goodenough, J. Electrochem. Soc. 144 (1997) 1188–1194.
[9] A. Manthiram, J.B. Goodenough, J. Solid State Chem. 71 (1987) 349–360.
[10] A. Manthiram, J.B. Goodenough, J. Power Sources 26 (1989) 403–408.
[11] A. Manthiram, Electrochem. Soc. Interface 18 (1) (2009) 44–47.
[12] N. Recham, J.-N. Chotard, L. Dupont, C. Delacourt, W. Walker, M. Armand, J.-M. Tarascon, Nat. Mater. 9 (2010) 68–74.
[13] M. Morcrette, P. Rozier, L. Dupont, E. Mugnier, L. Sannier, J. Galy, J.-M. Tarascon, Nat. Mater. 2 (2003) 755–761.
[14] P. Rozier, M. Morcrette, O. Szajwaj, V. Bodenez, M. Dolle, C. Surcin, L. Dupont, J.-M. Tarascon, Israel J. Chem. 48 (2008) 235–249.
[15] M. Giorgetti, S. Mukerjee, S. Passerini, J. McBreen, W.H. Smyrl, J. Electrochem. Soc. 148 (7) (2001) A768–A774.
[16] J.-S. Chung, H.-J. Sohn, J. Power Sources 108 (2002) 226–231.
[17] C. Masquelier, P. Reale, C. Wurm, M. Morcrette, L. Dupont, D. Larcher, J. Electrochem. Soc. 149 (2002) A1037–A1044.
[18] P. Poizot, E. Baudrin, S. Laruelle, L. Dupont, M. Touboul, J.-M. Tarascon, Solid State Ionics 138 (2000) 31–40.
[19] A.S. Aricò, P. Bruce, B. Scrosati, J.-M. Tarascon, W. Van Schalkwijk, Nat. Mater. 4 (2005) 366–377.
[20] P.G. Bruce, B. Scrosati, J.-M. Tarascon, Angew. Chem. Int. 47 (2008) 2930–2946.
[21] B. Kattouf, G.L. Frey, A. Siegmann, Y. Ein-Eli, Chem. Commun. (2009) 7396–7398.
[22] D. Kovacheva, B. Markovsky, G. Salitra, Y. Talyossef, M. Gorova, E. Levi, M. Riboch, H.-J. Kim, D. Aurbach, Electrochim. Acta 50 (2005) 5553–5560.
[23] K. Heinzinger, B. Maiwald, Bull. Chem. Soc. Jpn. 45 (1972) 2237–2239.
[24] A. Reisman, J. Karlak, J. Am. Chem. Soc. 80 (24) (1959) 6500–6503.
[25] J. Hume, J. Colvin, Proc. R. Soc. Lond. A 132 (820) (1931) 548–560.
[26] D. Aurbach, B. Markovsky, G. Salitra, E. Markevich, Y. Talyossef, M. Koltypin, L. Nazar, B. Ellis, D. Kovacheva, J. Power Sources 165 (2007) 491–499.
[27] P. Podhajecky, B. Scrosati, J. Power Sources 16 (1985) 309–317.
[28] N.A. Godshal, Solid State Ionics 18–19 (1986) 788–793.